Wireless Networks 8, 443–454, 2002

Exposure in Wireless Sensor Networks: Theory and Practical Solutions

SEAPAHN MEGERIAN
4532 Boelter Hall, UCLA Computer Science Department, Los Angeles, CA 90095, USA

FARINAZ KOUSHANFAR
545T Cory Hall (DOP Center) EECS Department, UC Berkeley, Berkeley, CA 94720, USA

GANG QU
1417 A.V. Williams, College Park, MD 20742, USA

GIACOMINO VELTRI and MIODRAG POTKONJAK
4532 Boelter Hall, UCLA Computer Science Department, Los Angeles, CA 90095, USA

Abstract. Wireless ad hoc sensor networks have the potential to provide the missing interface between the physical world and the Internet, thus impacting a large number of users. This connection will enable computational treatments of the physical world in ways never before possible. In this far reaching scenario, Quality of Service can be expressed in terms of accuracy and/or latency of observing events and the overall state of the physical world. Consequently, one of the fundamental problems in sensor networks is the calculation of coverage, which can be defined as a measure of the ability to detect objects within a sensor filed. Exposure is directly related to coverage in that it is an integral measure of how well the sensor network can observe an object, moving on an arbitrary path, over a period of time. After elucidating the importance of exposure, we formally define exposure and study its properties. We have developed an efficient and effective algorithm for exposure calculations in sensor networks, specifically for finding minimal exposure paths. The minimal exposure path provides valuable information about the worst case exposure-based coverage in sensor networks. The algorithm can be applied to any given distribution of sensors, sensor and sensitivity models, and characteristics of the network. Furthermore, it provides an unbounded level of accuracy as a function of run time and storage. Finally, we provide an extensive collection of experimental results and study the scaling behavior of exposure and the proposed algorithm for its calculation.

Keywords: wireless, sensor, network, exposure, coverage

1. Introduction

1.1. Motivation

Recent convergence of technological and application trends have resulted in exceptional levels of interest in wireless ad hoc networks and in particular wireless sensor networks. The push was provided by rapid progress in computation and communication technology as well as the emerging field of low cost, reliable, MEMS-based sensors. The pull was provided by numerous applications that can be summarized under the umbrella of computational worlds, where the physical world can be observed and influenced through the Internet and wireless sensor network infrastructures. Consequently, there have been a number of vigorous research and development efforts at all levels of development and usage of wireless sensor networks, including applications, operating systems, architectures, middleware, integrated circuit, and system. In many cases, the techniques and tools from general purpose and/or DSP computing can be adopted to the new scenarios with some modifications and generalizations. However, a number of technical challenges are unique in wireless sensor networks. Wireless sensor networks pose a number of fundamental problems related to their deployment, location discovery, and tracking, among which, exposure has a special place and role. Exposure can informally be described as the expected average ability of observing a target moving in a sensor field. More formally exposure can be defined as an integral of a sensing function that generally depends on distance from sensors on a path from a starting point p_S to destination point p_D. The specific sensing function parameters depend on the nature of the sensor device and the environment. A common model used in practice for omnidirectional sensors (such as seismic sensors) has the from αd^{-K}, with K typically ranging from 1 to 4.

The difficulty, complexity, and beauty of the exposure problem can be illustrated using a very simple, yet nontrivial problem illustrated in figure 1. The task is to find a path with minimal exposure for an object traveling from the point p_S to the point p_D. The field has a single sensor node s, located at the intersection of the diagonals of the square field F. The sensor s senses the object with sensitivity that is inversely proportional to the distance between the object and s.

Meguerdichian et al. [24] propose an algorithm for calculating the maximal breach path in a sensor network. The

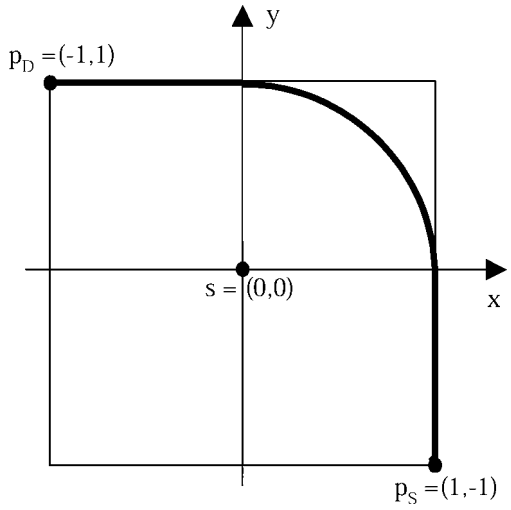

Figure 1. Exposure example.

maximal breach path is defined as a path where its closest distance to any sensor is as large as possible. The key idea there is to use the Voronoi diagram of the sensor nodes as a set of piecewise linear components to limit the search space for optimal paths. The Voronoi diagram is formed from lines that bisect and are perpendicular to the lines that connect two neighboring sensors. For finding maximal breach paths, it is advantageous to move along the lines of the Voronoi diagram, since stepping away from the Voronoi lines will ensure that at least one sensor is closer to the path. At first glance, it may seem that for minimization of exposure, it is also beneficial to follow the edges of the Voronoi diagram. However, as we will prove in section 4, this intuition is not true. For our simple example, we show the minimal exposure path (bold) in figure 1. Interestingly, the optimal path in this case partially, but not completely uses the edges of the bounded Voronoi diagram. From this example, we can observe that it is at times beneficial to deviate from Voronoi edges and step closer to sensors and still reduce the overall exposure, due to the reduced sensing time and shorter path length. In section 4, we revisit and discuss the details of this exposure problem.

1.2. Research goals and applications of exposure

We have a number of strategic objectives in mind. The first is a comprehensive and more importantly sound treatment of the exposure problem. Our goal is to provide formal, yet intuitive formulations, establish the complexity of the problem and to develop practical algorithms for exposure calculation that are suitable for implementation on platforms with limited resources. The next objective is to study the relationship and interplay of exposure with other fundamental wireless sensor network tasks, and in particular with location discovery and deployment. More specifically, we study how errors in location discovery impact the calculation of exposure and how one may statistically predict the required number of sensors for a targeted level of exposure.

In addition to strategic goals, we also have several technical and optimization objectives. Our main goal here is to establish techniques that bridge the gap between continuous-domain coverage problems and discrete mathematical objects. It is important to emphasize that in addition to exposure related problems, many other wireless sensor network problems intrinsically have both continuous and discrete components. Furthermore, our goal is to apply statistical techniques to study scaling, stability, and error propagation in wireless sensor network problems.

Besides the theoretic treatment of exposure, we opt to focus on at least one application, namely finding the minimal exposure path, in order to concretize and illustrate the utility of exposure. Computing and analyzing minimal exposure paths not only facilitates better understanding of exposure and how it behaves, but also provides a solid framework in answering the primary sensor coverage question: *How well can the sensors observe the field?* By being able to compute the minimal exposure path connecting given points p_S and p_D we can establish a coverage level guarantee since no object traveling on *any* path connecting p_S and p_D can have lower exposure to sensors. As one can infer from this statement, exposure is directly related to the likelihood of detection by sensors in that, higher exposure levels indicate higher chances of being observed by the sensors. In order to establish the significance of the minimal exposure path, let us consider a battle field scenario where multiple seismic sensors are scattered across a field in an attempt to detect enemy activity. Even in the most unlikely event that the enemy can guess the locations of every sensor node, the best it can do to avoid detection is to travel along the minimal exposure path. Of course, in battles and also in most realistic deployment scenarios, at least some sensors will be prone to fail either due to reserve energy depletion, malfunction, hostile attacks, or other events. Therefore, algorithms designed for performing such computation must be robust enough to handle frequent and unexpected changes in network topology.

Clearly, minimal exposure path is not the only useful application of exposure. In many instances computing average and expected exposure levels of agents moving in a sensor field can provide practical information on coverage levels and the overall quality of service of the network. Not only can exposure information be useful in managing and optimizing the network, it can also be used to guide the actions of agents in the field, governed by a judiciously selected set of objective functions. Furthermore, the applicability of exposure is not simply restricted to sensor networks. For instance, given the positions of a set of radio frequency (RF) transmitters in a field, exposure can be used to determine the expected quality of service (reception) along a specific path in the field. Also, since mobile agents in a field often have limited energy reserves for transmission and reception, exposure calculations can guide agent movements in such a way that communication energy requirements are minimized.

1.3. Organization

The reminder of this article is organized in the following way. First, we briefly survey the related work. Then, in order to

make the discussion self-contained, we summarize technical preliminaries and some background information, as well as provide the formal definition of exposure. Next, in section 4, we present analytical discussions and results on exposure and discuss several properties. In section 5, we present an efficient algorithm for exposure calculation specifically targeted for finding minimal exposure paths. In section 6, we present extensive, statistically validated, experimental results, followed by the conclusions.

2. Related work

Both coverage and wireless sensor networks are intrinsically multidisciplinary research topics. Therefore, a wide body of scientific and technological work is related to the research presented in this paper. In this section, we briefly cover only the most directly related areas: sensors, wireless ad hoc sensor networks, the coverage problem, related sensor network problems such as location discovery and deployment, and numerical analysis techniques.

2.1. Sensors

A sensor is a device that produces a measurable response to a change in a physical condition, such as temperature, magnetic field, and light. Although sensors have been around for a long time, two recent technological revolutions have greatly enhanced their importance and their range of application. The first was the connection of sensors to computer systems while the second was the emergence of MEMS sensors with their small size, small cost, and high reliability. There are a number of comprehensive surveys for a variety of sensor systems, including [5,23,26,37]. A more mathematical treatment of sensors with focus on their computer science aspects can be found in [21].

2.2. Wireless ad hoc sensor networks

Lansford and Bahl [19] and Haartsen and Mattisson [14] provide two examples of technologies where wireless sensor networks have been attracting a great deal of commercial and research interest. The practical emergence of such wireless ad hoc networks is widely considered revolutionary both in terms of a paradigm shift as well as an enabler of new applications. In ad hoc networks, no fixed network infrastructure exists (as opposed to cellular phone networks for instance). Hence, they can be adapted and deployed much more rapidly. Furthermore, integration of inexpensive, power efficient and reliable sensors in nodes of wireless ad hoc networks, with significant computational and communication resources, has opened new research and engineering vistas. A number of high-profile applications for wireless sensor networks have been proposed such as [33] and [10]. The applications range from connecting the internet to the physical world to creating new proactive environments. At the same time, wireless sensor networks pose a number of demanding new technical problems, including the need for new DSP algorithms [28], operating systems [4], low power designs [2], and integration with biological systems [1].

2.3. Coverage problems

Several different coverage formulations arise naturally in many domains. The Art Gallery Problem, for example, deals with determining the number of observers necessary to cover an art gallery room such that every point is seen by at least one observer. It has found several applications in many domains such as for optimal antenna placement problems in wireless communication. The Art Gallery problem was solved optimally in 2D and was shown to be NP-hard in the 3D case. Marengoni et al. [22] propose heuristics for solving the 3D case using Delaunay triangulations. Kang and Golay [17] describe a general systematic method for developing an advanced sensor network for monitoring complex systems such as those found in nuclear power plants, but do not present any general coverage algorithms. Sensor coverage for detecting global ocean color where sensors observe the distribution and abundance of oceanic phytoplankton is approached by assembling and merging data from satellites at different orbits as presented in [13]. Coverage studies to maintain connectivity have been the focus of study for many years. For example, Molina et al. [25] and Lieska et al. [20] calculate the optimum number of base stations required to achieve service objectives. In some instances, connectivity is achieved through mobile host attachments to a base station. However, the connectivity coverage is more important in the case of ad hoc wireless networks since the connections are peer-to-peer. Haas [15] shows the improvement in network coverage due to multi-hop routing capabilities and optimizes the coverage constraint subject to a limited path length.

As mentioned earlier, Meguerdichian et al. [24] present several formulations of coverage in sensor networks. These formulations include the best- and worst-case coverage for agents moving in a sensor field, characterized by maximal breach and maximal support paths respectively. There, distances to the closest sensors are of importance, while in the exposure-based method presented here, the detection probability (observability) in the sensor field is characterized and computed as a path dependent integral of multiple sensor intensities.

2.4. Related sensor network problems: Location discovery and deployment

Location discovery is a fundamental task in many ad hoc wireless networks, especially sensor networks. There are three separate, yet related steps in the this process: (i) measurement, (ii) algorithmic location discovery procedure, and (iii) confidence (error) calculation. While the first two steps have been extensively addressed in the past, the literature on the last phase is relatively scarce. During measurement one or more characteristics of wireless signals are measured in order to establish the distance between the transmitter and re-

ceiver. The techniques proposed for these measurements often include received signal strength indicator (RSSI), time-of-arrival (ToA), time-difference-of-arrival (TDoA), and angle-of-arrival (AoA) [12].

Procedures for algorithmic location discovery can be classified in two large groups: those used in fixed infrastructure wireless systems and those in wireless ad hoc systems. While the first group has been an active area of research and development for a long time, the second group has only recently become the focus of intense study. In the first group, most notable location discovery systems include AVL [30,35], Loran [31], GPS [6,11], systems used by cellular base stations for tracking of mobile users [7,8], the Cricket location discovery systems [27], and active badge systems [36]. A number of location discovery systems have been proposed. For the sake of brevity, we refer to the comprehensive comparative survey and detailed discussion on a number of wireless ad hoc network location discovery systems and techniques presented in [18].

2.5. Numerical algebra and analysis

There are two main questions related to numerical computation of integrals that are not defined in closed formula form: error accumulation and applied method of integration. It is well known that numerical error accumulation and propagation is an intractable problem for all but the simplest cases [3,34]. Therefore, we opt to analyze numerical errors using statistical techniques [29,34]. For integration, there is a wide spectrum of applicable techniques such as those presented in [16,32]. In our experiments, we use the relatively simple trapezoidal method. Some alternatives include the *Gauss–Kronrod* and *adaptive quadrature* algorithms [16]. While such techniques reduce calculation errors, they are significantly more computationally intensive. Also, their advantage is most prevalent in cases where functions vary rapidly. Our experiments indicate that this is very rarely the case in calculations of exposure in wireless sensor networks.

3. Technical preliminaries

3.1. Sensor models

Sensing devices generally have widely different theoretical and physical characteristics. Hence, numerous models of varying complexity can be constructed based on application needs and device features. Interestingly, most sensing device models share two facets in common:

(1) Sensing ability diminishes as distance increases.

(2) Due to diminishing effects of noise bursts in measurements, sensing ability can improve as the allotted sensing time (exposure) increases.

For the sake of exposure calculations, the only requirement that we pose is that sensor sensibility at each point in the field must be *defined* and *non-negative*. Having this in mind, for a sensor s, we express the general sensibility model S at an arbitrary point p as

$$S(s, p) = \frac{\lambda}{[d(s, p)]^K},$$

where $d(s, p)$ is the Euclidean distance between the sensor s and the point p, and positive constants λ and K are sensor technology-dependent parameters. Although our mild requirement on sensor sensibility facilitates the formulation and use of a wide array of sensing models, we focus our subsequent discussions on this model due to its wide range of applicability to existing technologies.

3.2. Sensor field intensity and exposure

In order to introduce the notion of exposure in sensor fields, we first define the *Sensor Field Intensity* for a given point p in the sensor field F. Depending on the application and the type of sensor models at hand, the sensor field intensity can be defined in several ways. Here, we present two models for the sensor field intensity: *All-Sensor Field Intensity* (I_A) and *Closest-Sensor Field Intensity* (I_C).

Definition. *All-Sensor Field Intensity* $I_A(F, p)$ for a point p in the field F is defined as the effective sensing measures at point p from all sensors in F. Assuming there are n active sensors, $s_1, s_2, \ldots, s_n$, each contributing with the sensibility function S, I_A is expressed as

$$I_A(F, p) = \sum_{1}^{n} S(s_i, p).$$

Definition. *Closest-Sensor Field Intensity* $I_C(F, p)$ for a point p in the field F is defined as the sensing measure at point p from the closest sensor in F, i.e. the sensor that has the smallest Euclidean distance from point p. I_C is expressed as

$$s_{\min} = s_m \in S \mid d(s_m, p) \leqslant d(s, p)\ \forall s \in S,$$
$$I_C(F, p) = S(s_{\min}, p),$$

where $s_{\min}$ is the closest sensor to p.

Suppose an object O is moving in the field F from point $p(t_1)$ to point $p(t_2)$ along the curve (or path) $p(t)$. We now define the exposure of this movement.

Definition. The *exposure* for an object O in the sensor field during the interval $[t_1, t_2]$ along the path $p(t)$ is defined as

$$E\big(p(t), t_1, t_2\big) = \int_{t_1}^{t_2} I\big(F, p(t)\big)\left|\frac{\mathrm{d}p(t)}{\mathrm{d}t}\right| \mathrm{d}t,$$

where the sensor field intensity $I(F, p(t))$ can either be $I_A(F, p(t))$ or $I_C(F, p(t))$ and $|\mathrm{d}p(t)/\mathrm{d}t|$ is the element of arc length. For example, if $p(t) = (x(t), y(t))$, then

$$\left|\frac{\mathrm{d}p(t)}{\mathrm{d}t}\right| = \sqrt{\left(\frac{\mathrm{d}x(t)}{\mathrm{d}t}\right)^2 + \left(\frac{\mathrm{d}y(t)}{\mathrm{d}t}\right)^2}.$$

4. Exposure

We start our discussion on exposure by considering the simplest case. There is only one sensor at position $(0, 0)$ whose sensibility function at point $p(x, y)$ is defined as

$$S\big(s(0,0),\, p(x,y)\big) = \frac{1}{d(s,p)} = \frac{1}{\sqrt{x^2+y^2}}.$$

We study the problem of how to travel from point $p(1, 0)$ to point $q(X, Y)$ with the minimum exposure, i.e. finding continuous functions $x(t)$ and $y(t)$, such that $x(0) = 1$, $y(0) = 0$; $x(1) = X$, $y(1) = Y$; and

$$E = \int_0^1 \frac{1}{\sqrt{x(t)^2+y(t)^2}} \sqrt{\left(\frac{\mathrm{d}x(t)}{\mathrm{d}t}\right)^2 + \left(\frac{\mathrm{d}y(t)}{\mathrm{d}t}\right)^2}\,\mathrm{d}t$$

is minimized. Note that here we are using the *closest-sensor* (I_C) intensity model.

Lemma 1. If $q = (0, 1)$, then the minimum exposure path is $(\cos \pi t/2, \sin \pi t/2)$, and the exposure along this path is $E = \pi/2$.

Proof. Consider the lines that start from the origin, where sensor s is located, and intersect the x-axis, where the object is located, at angle α_i, such that

$$0 < \alpha_1 < \cdots < \alpha_i < \alpha_{i+1} < \cdots < \alpha_n = \frac{\pi}{2}.$$

Clearly, the path from point $p(1, 0)$ to $q(0, 1)$ with minimum exposure will intersect each line in order and only once. Let p_i be the intersection point. We use the line segments $p_i p_{i+1}$ to approximate the path between points p_i and p_{i+1}.

Draw lines perpendicular to line segments $p_i p_{i+1}$ from origin s and name the intersection point s_i. We further denote the angles $\angle p_i s s_i$ and $\angle s_i s p_{i+1}$ by β_i and γ_i as shown in figure 2.

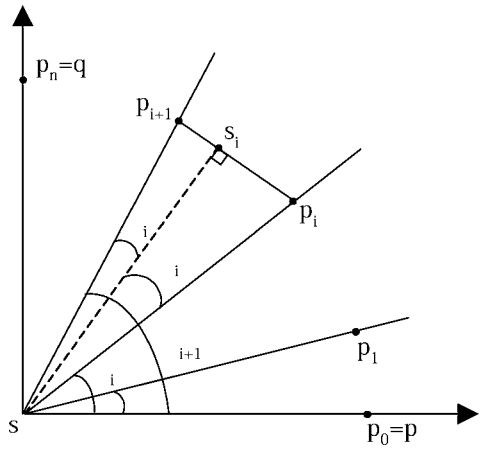

Figure 2. Proof for lemma 1.

One can verify that the exposure from p_i to s_i along the line segment is

$$\int_0^{l\sin\beta_i} \frac{1}{\sqrt{l^2\cos^2\beta_i + x^2}}\,\mathrm{d}x = \ln\frac{1+\sin\beta_i}{\cos\beta_i},$$

where l is the distance between points s and p_i. Therefore, the exposure of traveling from point p_i to p_{i+1} is

$$\ln\frac{1+\sin\beta_i}{\cos\beta_i} + \ln\frac{1+\sin\gamma_i}{\cos\gamma_i}.$$

Notice that since $\beta_i + \gamma_i = \alpha_{i+1} - \alpha_i$, which is a constant for a given set of

$$0 < \alpha_1 < \cdots < \alpha_i < \alpha_{i+1} < \cdots < \alpha_n = \frac{\pi}{2},$$

we have that this exposure is minimized if and only if $\beta_i = \gamma_i$. This implies that $d(s, p) = d(s, q)$. In other words, to reach the $(i + 1)$th line (the one that intersects the x-axis with angle α_{i+1}) from point p_i, the best way is to move towards point p_{i+1}, the point that has the same distance from the sensor as p_i does.

As $n \to \infty$, we conclude that if the destination point $q = (0, 1)$, then the minimum exposure path is the quarter circle from $p = (1, 0)$ to $q = (0, 1)$ with center $(0, 0)$ and radius 1. This path can be expressed as

$$\left(\cos\frac{\pi}{2}t, \sin\frac{\pi}{2}t\right) \quad (0 \leqslant t \leqslant 1).$$

Thus, the exposure is

$$E = \int_0^1 \frac{1}{\sqrt{\cos^2(\pi t/2) + \sin^2(\pi t/2)}} \times \sqrt{\left(-\frac{\pi}{2}\sin\left(\frac{\pi}{2}t\right)\right)^2 + \left(\frac{\pi}{2}\cos\left(\frac{\pi}{2}t\right)\right)^2}\,\mathrm{d}t = \frac{\pi}{2}. \;\square$$

Notice that in the above proof, it is not necessary to have the starting point and ending point at $(1, 0)$ and $(0, 1)$. The only fact we utilize is that they have the same distance to the sensor. In general, we have:

Lemma 2. Given a sensor s and two points p and q, such that $d(s, p) = d(s, q)$, then the minimum exposure path between p and q is the arc that is part of the circle centered s and passing through p and q.

Now we study the minimum exposure path in a restricted region. We start with the case where the sensor is at the center of the square $|x| \leqslant 1$, $|y| \leqslant 1$.

Theorem 3. Let the sensor be located at $(0, 0)$ and the field restricted to the region $|x| \leqslant 1$, $|y| \leqslant 1$. The minimum exposure path from point $p(1, -1)$ to point $q(-1, 1)$ consists of three parts: a line segment from p to $(1, 0)$, a quarter circle from $(1, 0)$ to $(0, 1)$, and a line segment from $(0, 1)$ to q.

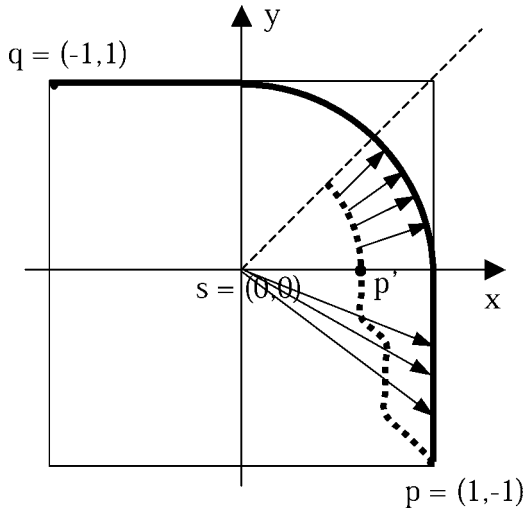

Figure 3. Proof for theorem 3.

Proof. By symmetry, we only need to prove that the minimum exposure path from point $p(1,-1)$ to dashed line $y = x$ is the line segment from $(1,-1)$ to $(1,0)$ followed by the arc centered at $(0,0)$ as shown in bold in figure 3. We show that this path has less exposure than any other continuous curve from $(1,-1)$ to the line $y = x$.

Let the dotted curve in figure 3 be an arbitrary curve connecting point $p(1,-1)$ and any point on the line $y = x$. Suppose it intersects the x-axis at point p'. From lemma 2, we know that the minimum exposure path from point p' to the line $y = x$ is the one that follows the circle centered at $(0,0)$ from p' to the dashed line $y = x$. Therefore, the dotted curve should include this arc. The exposure along this arc is $\pi/4$, same as that along the arc in bold from $(1,0)$ to line $y = x$. However, exposure along the dotted curve from p to p' is larger than that along the straight line segment from p to $(1,0)$ for two reasons: (1) the sensor is more sensitive to the points on the former curve because they are closer to the sensor; (2) the length of the former curve is longer than the latter, which is the shortest from p to the x-axis. Therefore, traveling along the dotted curve induces more exposure than the bold curve, the minimum exposure path. □

We can extend this result to the case where the sensor field is a convex polygon and the sensor is at the center of the inscribed circle.

Let $v_1 v_2 \ldots v_i \ldots v_n$ be a polygonal field, s be the sensor, and edge $v_i v_{i+1}$ is tangent to the inscribed circle at point u_i as shown in figure 4. Define curves:

$$\Gamma_{ij} = \overline{v_i u_i} * \overbrace{u_i u_{i+1}} * \overbrace{u_{i+1} u_{i+2}} * \cdots * \overbrace{u_{j-2} u_{j-1}} * \overline{u_{j-1} v_j}$$

and

$$\Gamma'_{ij} = \overline{v_i u_{i-1}} * \overbrace{u_{i-1} u_{i-2}} * \overbrace{u_{i-2} u_{i-3}} * \cdots * \overbrace{u_{j+1} u_j} * \overline{u_j v_j},$$

where $\overline{u_i v_i}$ is the line segment from point u_i to point v_i, $\overbrace{u_i u_{i+1}}$ is the arc on the inscribed circle between the two points that does not pass any other u'_js, $*$ is the concatenation, and all $+/-$ operations are modulus n. Notice that if vertices

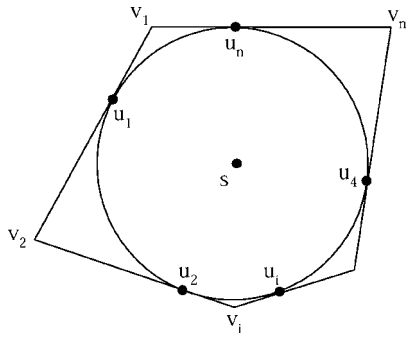

Figure 4.

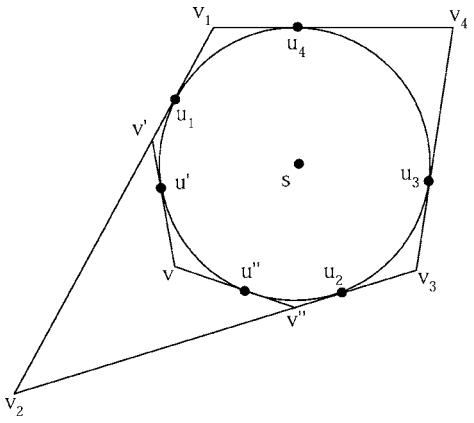

Figure 5.

v_i and v_j are adjacent, one of these two curves becomes edge $v_i v_j$. We have:

Corollary 4. The minimum exposure path from vertices v_i to v_j is either Γ_{ij} or Γ'_{ij} whichever has less exposure.

Define the corner at a vertex v_i as the area enclosed be curve $\overline{v_i u_i} * \overbrace{u_i u_{i-1}} * \overline{u_{i-1} v_i}$, i.e. the region that is inside the polygon but outside the inscribed circle. From any point v in a corner other than the vertex v_i, we draw two lines tangent to the circle: vv' that intersects edge $v_{i-1} v_i$ at v' and is tangent to circle at u'; and vv'' that intersects edge $v_i v_{i+1}$ at v'' and is tangent to circle at u''. Figure 5 shows this in a quadrilateral $v_1 v_2 v_3 v_4$ and its inscribed circle centered at s. Consider point v in the corner at vertex v_2. We want to find the minimum exposure path from v to a point in another corner, for example, vertex v_4, in the quadrilateral field. After drawing the two tangent lines vv' and vv'', this problem is reduced to finding such a path in a smaller convex polygon $v_1 v' v v'' v_3 v_4$, which is solvable by corollary 4. So we have:

Corollary 5. We can determine the minimum exposure path from one corner to another in a convex polygon.

However, the problem of finding the minimum exposure path between two points belonging to the same corner or when both are inside the inscribed circle (unless they are equidistant to the sensor) remains open.

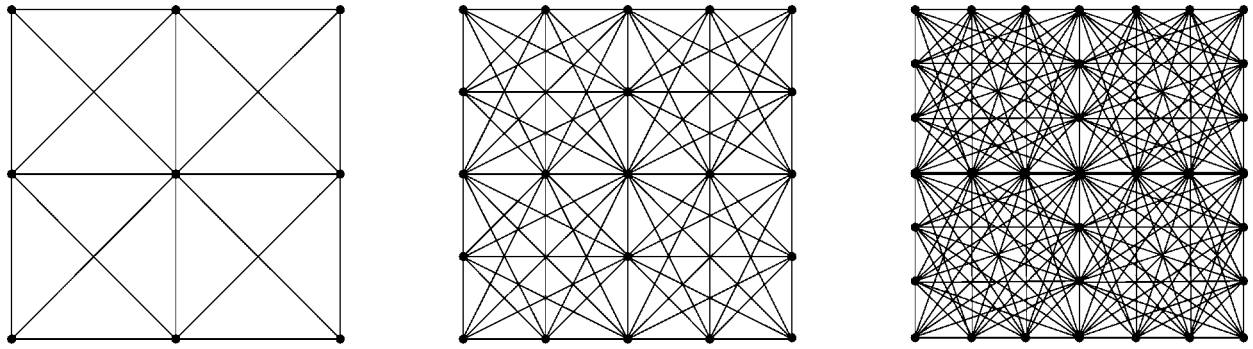

(a) n=2, m=1 (b) n=2, m=2 (c) n=2, m=3

Figure 6. First-order (a), second-order (b), and third-order (c) 2×2 generalized grid examples.

5. Generic approach for calculating minimal exposure path

As shown in section 4, it is possible to obtain analytic solutions to several simple instances of the exposure problem. However, finding the *minimum exposure path* in sensor networks under arbitrary sensor and intensity models is an extremely difficult optimization task. In this section we present a generic algorithm and several heuristics that can be used to obtain the solution to the exposure based coverage problem.

The generic exposure problem domain is continuous and the exposure expression often does not have an analytic, closed form, solution. To address these characteristics, the algorithm we propose here has three main parts:

(1) transform the continuous problem domain to a discrete one;

(2) apply graph-theoretic abstraction;

(3) compute the *minimal exposure path* using Dijkstra's Single-Source-Shortest-Path algorithm [9].

To transform the problem domain to a tractable discrete domain we use a generalized grid approach. For the sake of clarity, we restrict our subsequent discussion to the 2D case, however, the technique can easily be generalized to the 3D case.

In the grid-based approach, we divide the sensor network region using an $n \times n$ square grid and limit the existence of the *minimal exposure path* within each grid element. In the simplest case, the path is forced to exist only along the edges and the diagonals of each grid square as shown in figure 6(a). We call this case the *first-order* grid. However, since the minimal exposure path can travel in arbitrary directions through the sensor field, it is easy to see that the *first-order* grid creates significant inaccuracies in the final results since it only allows horizontal, vertical, and diagonal movements. We use higher order grid structures such as the *second-order* and *third-order* grids shown in figure 6(b) and (c) to improve the accuracy of the final solution. As can be deduced from figure 6, to construct the *mth-order* grid, we place $m + 1$ equally spaced vertices along each edge of a grid square. The *minimal exposure path* is then restricted to straight line segments connecting any two of the vertices in each square. It is easy to verify that as $n \to \infty$ and $m \to \infty$, the solutions produced by the algorithm approaches the optimum, at the cost of run-time and storage requirements.

Procedure *Minimal_Exposure_Path*(F, p_S, p_D) {
  $F_D(V, L) = Generate\_Grid(F, n, m)$
  Init Graph $G(V, E)$
  For all $v_i \in F_D$
    Add vertex v_i' to G

  For all $l_i(v_j, v_k) \in L$
    Add edge $e_i(v_j', v_k')$ to G
    $e_i \cdot weight = Exposure(l_i)$

  $vs =$ *find closest vertex to* p_S
  $ve =$ *find closest vertex to* p_D
  $Min\_Exposure\_Path = Single\_Source\_Shortest\_Path(G,vs,ve)$
}

Figure 7. Pseudo-code for finding the minimal exposure path in a sensor field F, given start point p_S and end point p_D.

The details of the algorithm are listed in figure 7. After generating the grid F_D, the next step is to transform F_D to the edge-weighted graph G. This is accomplished by adding a vertex in G corresponding to each vertex in F_D and an edge corresponding to each line segment in F_D. Each edge is assigned a weight equal to the exposure along its corresponding edge in F_D, calculated or approximated by the *Exposure*( ) function. This function calculates the exposure along the line segment using numerical integration techniques and can be implemented in a variety of ways. In our implementation, we use the simple trapezoidal rule in this function. As the pseudo-code in figure 7 shows, we use Dijkstra's Single-Source-Shortest-Path algorithm to find the minimal exposure path in G from the given source p_S to the given destination p_D. This step can be replaced by the Floyd–Warshal All-Pair-Shortest-Path algorithm to find the minimal exposure path between any arbitrary starting and ending points on the grid F_D. These two algorithms are well known and [9] provides a detailed discussion on both.

When the start- and end-points of the path are initially known, the run-time of the algorithm is generally dominated

by the grid generation process which has a linear run time over $|F_D|$, the total number of vertices in the grid. For an $n \times n$ grid with m divisions per edge, $|F_D| = n^2(2m-1)+2nm+1$ total grid points which means that the complexity of the algorithm is $O(n^2m)$ in the worst case. However, if the Single-Source-Shortest-Path algorithm is replaced by the All-Pair-Shortest-Path algorithm, then the run-time of the entire process is dominated by the shortest path calculation which has a complexity of $O(|F_D|^3)$.

6. Experimental results

In order to gain a deeper understanding of the exposure and exposure-based coverage in sensor networks, we have performed a wide range of simulations and case-studies. In this section, we present several interesting results and discuss their implications and possible applications.

6.1. Simulation platform

The main simulation platform consists of a standalone C++ package. The visualization and user interface elements are currently implemented using Visual C++ and OpenGL libraries. The sensor field in all experiments is defined as a square, 1000 m wide. We have assumed a constant speed ($|\mathrm{d}p(t)/\mathrm{d}t| = 1$) in all calculations of the minimal exposure path. This assumption significantly simplifies the required computation and allows for more visually intuitive results that are essential for demonstration purposes. The grid resolution in all cases is also fixed and was experimentally determined. In most cases, a 32×32 grid with 8 divisions per grid-square edge ($n = 32$, $m = 8$) were sufficient in producing accurate results. Unless otherwise specified, in all cases we compute the minimal exposure path between opposite corners of the field.

6.2. Uniformly distributed random sensor deployment

To create random sensor placements, we use two uniform random variables X and Y to compute the coordinates (x_i, y_i) of each sensor s_i in the field. The results in tables 1 and 2 show the mean, median, and standard deviation (σ) of exposure and path length calculated for 50 such cases. Table 1 lists results for varying number of sensors using the $1/d^2$ ($K = 2$) model and table 2 lists the results for the $1/d^4$ ($K = 4$) sensing model. Both tables include results for the I_A and I_C intensity models.

As tables 1 and 2 show, generally for sparse fields, there are a wide range of minimal exposure paths that can be expected from uniform random deployments. As sensor density increases in the field, the minimal exposure value and path lengths tend to stabilize. This effect can be observed in figure 8 that shows the relative standard deviation of exposure as the number of sensors increase. The results suggest that there is a saturation point after which randomly placing more sensors does not significantly impact the minimal exposure in the field. In our experiments we have observed that under

Table 1
Uniformly distributed random sensor deployment statistics for 50 instances using $1/d^2$ sensing model.

$K = 2$	Intensity model: All Sensors (I_A)						Intensity model: Closest Sensor (I_C)					
	Exposure			Path length (m)			Exposure			Path length(m)		
Sensors	Avg.	Med.	σ	Avg.	Med.	σ	Avg.	Med.	σ	Avg.	Med.	σ
23	0.29371	0.29364	0.043	1507.3	1537.9	258.3	0.07707	0.07386	0.023	1663.9	1671.9	205.7
26	0.33856	0.33542	0.051	1527.2	1538.0	269.0	0.08292	0.08200	0.024	1666.2	1673.5	214.4
27	0.35388	0.35310	0.054	1537.2	1607.1	280.7	0.08795	0.08490	0.023	1667.5	1688.2	228.5
74	1.21923	1.19378	0.133	1564.8	1576.2	229.2	0.22516	0.21827	0.049	1727.3	1757.3	169.8
79	1.29571	1.30208	0.130	1574.9	1558.9	245.8	0.23659	0.23168	0.046	1714.1	1700.0	183.3
85	1.43679	1.44794	0.127	1567.9	1568.1	203.4	0.25508	0.24577	0.049	1692.8	1689.8	181.8
119	2.18092	2.16669	0.147	1542.5	1552.7	233.2	0.35227	0.35154	0.056	1712.1	1707.6	155.2
126	2.32193	2.34368	0.176	1570.4	1577.5	209.3	0.36934	0.36404	0.059	1732.1	1702.4	151.8
146	2.78671	2.78598	0.202	1578.9	1595.3	196.1	0.42370	0.43267	0.059	1708.0	1714.1	121.6

Table 2
Uniformly distributed random sensor deployment statistics for 50 instances using $1/d^4$ sensing model.

$K = 4$	Intensity model: All Sensors (I_A)						Intensity model: Closest Sensor (I_C)					
	Exposure ($\times 10^{-5}$)			Path length (m)			Exposure ($\times 10^{-5}$)			Path length (m)		
Sensors	Avg.	Med.	σ	Avg.	Med.	σ	Avg.	Med.	σ	Avg.	Med.	σ
23	1.41637	0.95749	1.781	1617.6	1648.4	298.3	0.90822	0.43206	1.686	1753.4	1727.3	292.1
26	1.58834	1.10111	1.803	1718.7	1678.3	325.1	0.94988	0.51095	1.711	1807.6	1753.2	323.4
27	1.66767	1.19165	1.781	1678.6	1702.0	324.8	1.02837	0.61186	1.728	1726.9	1721.2	278.0
74	11.1643	8.99673	7.072	1777.1	1807.4	245.2	5.62326	3.79916	5.542	1881.0	1888.0	236.2
79	12.3447	10.3248	7.488	1730.7	1724.0	232.4	5.85618	4.19891	5.471	1833.4	1832.7	247.4
85	13.8395	11.9162	7.539	1696.0	1670.8	228.3	6.61165	4.96789	5.621	1838.0	1795.6	251.7
119	26.5454	23.3566	9.838	1783.6	1782.6	223.7	11.9136	9.45342	6.437	1872.5	1875.0	240.0
126	28.6042	26.7352	10.186	1776.0	1783.2	210.5	12.5021	10.9340	6.468	1902.7	1883.2	217.0
146	36.9259	34.6413	10.793	1755.4	1743.6	183.2	15.8885	14.0267	7.213	1861.8	1829.9	193.6

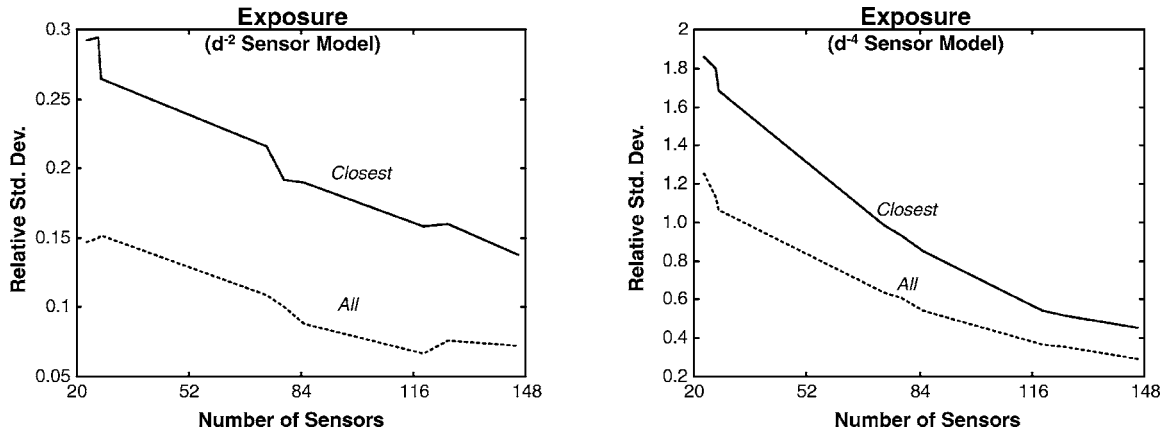

Figure 8. Diminishing relative standard deviation in exposure for $1/d^2$ and $1/d^4$ sensor models.

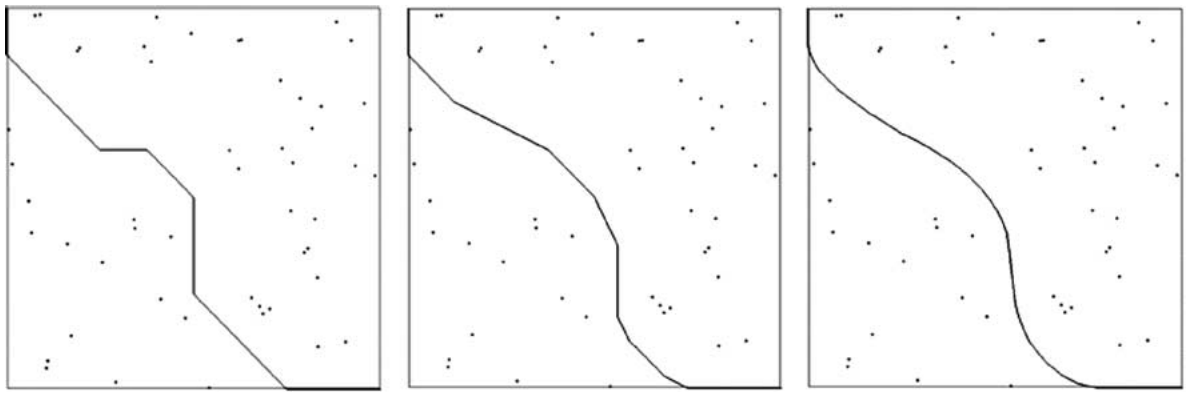

Figure 9. Minimum exposure path for 50 randomly deployed sensors under the All-Sensor intensity model (I_A) and varying grid resolutions: $n = 8$, $m = 1$ (left); $n = 16$, $m = 2$ (middle); $n = 32$, $m = 8$ (right).

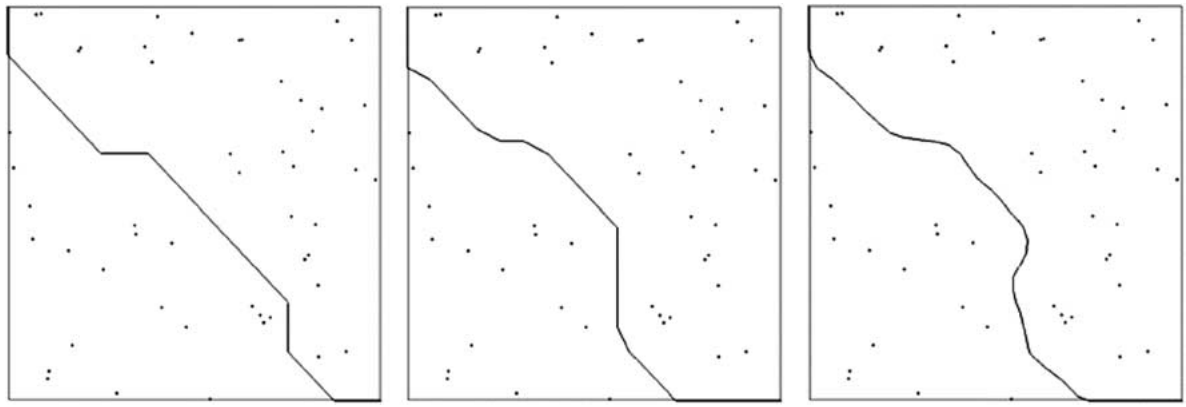

Figure 10. Minimum exposure path for 50 randomly deployed sensors under the Closest-Sensor intensity model (I_C) and varying grid resolutions: $n = 8$, $m = 1$ (left); $n = 16$, $m = 2$ (middle); $n = 32$, $m = 8$ (right).

the I_A intensity model, as the number of sensors increase, the minimal exposure path generally gets closer to the bounding edges of the field, and the path length approaches the half field perimeter value. This behavior is caused by the fact that sensors are only allowed to exist in the field and thus the boundary edges of the field are generally farther from the bulk of sensors.

Figures 9 and 10 show an instance of the minimal exposure path problem computed using grids with different resolutions. Shown are the solutions obtained for a low resolution 8×8 grid, a higher resolution 16×16 grid, and an ultra-high resolution 32×32 grid under the I_A and I_C intensity models. It is interesting to note that even when using the very low-resolution 8×8 grid, the calculated path is fairly close to the accurate paths obtained by the higher resolution grids.

6.3. Deterministic sensor placement

In addition to random deployments, we have studied the effects of several regular, deterministic sensor placement strate-

Table 3
Minimal exposure path results for several deterministic sensor deployment schemes.

Sensor model	d^{-2}				d^{-4}			
Intensity model	All		Closest		All		Closest	
Sensors	Exp.	Dist.	Exp.	Dist.	Exp. ($\times 10^{-5}$)	Dist.	Exp. ($\times 10^{-5}$)	Dist.
Cross (+)								
23	0.37921	1824.0	0.10534	1454.4	5.16387	1618.1	2.41489	1662.5
79	1.81619	1885.5	0.46292	1626.3	263.737	1620.9	138.652	1659.8
119	2.92691	1881.1	0.76240	1614.8	1076.93	1620.9	604.345	1655.5
Square								
23	0.29164	1471.5	0.08075	1692.9	0.95149	1594.0	0.41017	1771.3
79	1.53523	1452.6	0.35159	1688.5	17.3337	1613.2	7.40201	1835.4
119	2.58348	1451.4	0.55955	1687.7	42.8954	1618.3	18.2303	1901.7
Triangle								
27	0.41380	1730.6	0.12998	1713.3	1.92757	1785.3	1.04335	1783.4
85	1.73666	1890.8	0.43943	1711.7	22.5250	2081.2	11.6667	1757.5
126	2.78817	1917.6	0.65938	1708.4	51.3402	2010.2	26.2746	1775.7
Hexagon								
26	0.38024	1455.1	0.10515	1630.0	1.58610	1559.2	0.67755	1845.1
74	1.48514	1450.9	0.34277	1642.2	16.6052	1776.4	7.03031	1864.1
146	3.43761	1446.9	0.70736	1624.3	72.4104	1545.5	31.3033	1795.1

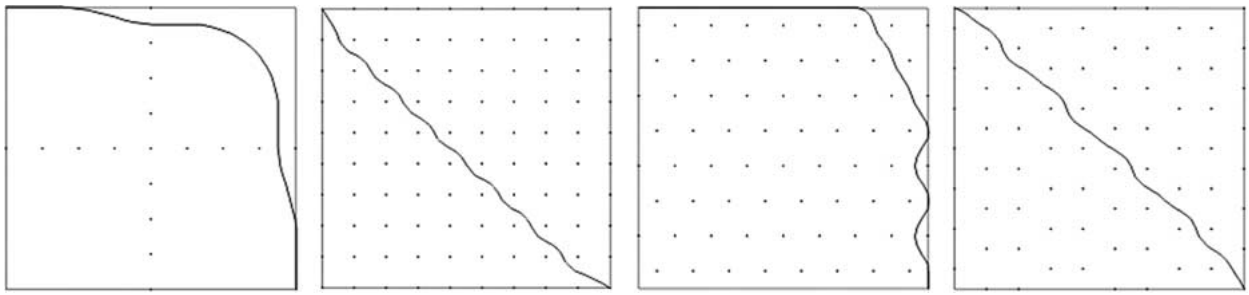

Figure 11. Minimum exposure path under the All-Sensor intensity model (I_{A}) using cross, square, triangle, and hexagon based deterministic sensor deployment schemes.

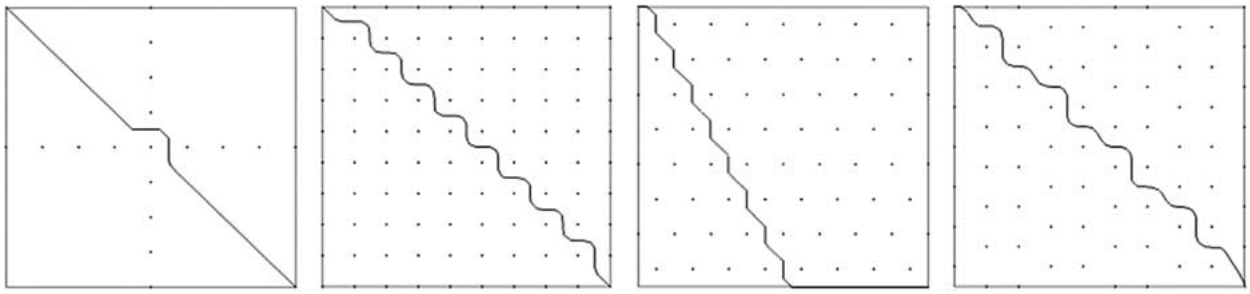

Figure 12. Minimum exposure path under the Closest-Sensor intensity model (I_{C}) using cross, square, triangle, and hexagon based deterministic sensor deployment schemes.

gies on exposure. Table 3 lists the exposure and path lengths for several such strategies of sensor deployment using the $1/d^2$ ($K = 2$) and $1/d^4$ ($K = 4$) sensing models, I_{A} and I_{C} intensity models, and varying number of sensors.

In the cross deployment scheme, sensors are equally spaced along the horizontal and vertical line that split the square field in half. In the square-based approach, sensors are placed at the vertices of a grid. In the triangle- and hexagon-based methods, sensors are placed at the vertices of equally spaced triangular and hexagonal partitions in the sensor field. Clearly, numerous other placements can be constructed, however, these four cases serve as a guide on how coverage in deterministic deployment scenarios can differ from random cases.

In our experiments the cross-based deployment scheme provided the best level of exposure followed by the triangle-based scheme. The hexagon- and square-based schemes also present several interesting characteristics. Figures 11 and 12 depict the deterministic deployment instances in action. Overall, the exposure along the minimal exposure path

for the cross-, triangle-, square-, and hexagon-based deployment schemes was higher than the average randomly generated network topology. Finding the optimal placements of sensors to guarantee exposure coverage levels is an interesting and challenging problem. For example, in certain instances it may be desirable to detect objects entering the field as soon as possible which may suggest placing sensors at the boundaries of the field. In other instances, more uniform coverage levels may be beneficial, suggesting the use of more uniform sensor deployment schemes such as the triangular and hexagonal deployment schemes.

7. Conclusion

Calculation of exposure is fundamental for coverage computation in wireless ad hoc sensor networks. We introduced exposure and the exposure-based coverage model, formally defined exposure, and studied several of its properties. Using a multiresolution technique and Dijkstra's and/or Floyd–Warshall's shortest path algorithms, we presented an efficient and effective algorithm for finding minimal exposure paths for any given distribution and characteristics of sensor networks. The algorithm works for arbitrary sensing and intensity models with the only assumption that sensor sensibilities are defined and non-negative at every point in the field. The algorithm provides an unbounded level of accuracy as a function of run time. Experimental results indicate that the algorithm can produce high quality results efficiently and can be utilized as a performance and worst-case coverage analysis tool in sensor networks.

Acknowledgements

This material is based upon work partially supported by the National Science Foundation under Grant No. NI-0085773 and DARPA and Air Force Research Laboratory under Contract No. F30602-99-C-0128. Any opinions, findings, conclusions, or recommendations expressed in this material are those of the authors' and do not necessarily reflect the views of the NSF, DARPA, or Air Force Research Laboratory.

References

[1] H. Abelson et al., Amorphous computing, Communications of the ACM 43(5) (May 2000) 74–82.
[2] A.A. Abidi, G.J. Pottie and W.J. Kaiser, Power-conscious design of wireless circuits and systems, Proceedings of the IEEE 88(10) (October 2000) 1528–1545.
[3] F.S. Acton, *Numerical Methods That Work* (Mathematical Association of America, Washington, DC, 1990).
[4] W. Adjie-Winoto, E. Schwartz, H. Balakrishnan and J. Lilley, The design and implementation of an intentional naming system, Operating Systems Review 33(5) (December 1999) 186–201.
[5] H. Baltes, O. Paul and O. Brand, Micromachined thermally based CMOS micro-sensors, Proceedings of the IEEE 86(8) (August 1998) 1660–1678.
[6] M.S. Braasch and A.J. Van Dierendonck, GPS receiver architectures and measurements, Proceedings of the IEEE 87(1) (January 1999) 48–64.
[7] J. Caffery Jr. and G.L. Stuber, Subscriber location in CDMA cellular networks, IEEE Transactions on Vehicular Technology 47(2) (May 1998) 406–416.
[8] J. Caffery Jr. and G.L. Stuber, Nonlinear multiuser parameter estimation and tracking in CDMA systems, IEEE Transactions on Communications 48(12) (December 2000) 2053–2063.
[9] T. Cormen, C. Leiserson and R. Rivest, *Introduction to Algorithms* (MIT Pres, 1990).
[10] D. Estrin, R. Govindan and J. Heidemann, Embedding the Internet: Introduction, Communications of the ACM 43 (May 2000) 38–42.
[11] S. Fisher and K. Ghassemi, GPS IIF – The next generation, Proceedings of the IEEE 87(1) (January 1999) 24–47.
[12] J.D. Gibson, *The Mobile Communications Handbook* (CRC Press, Boca Raton, IEEE Press, New York, 1996).
[13] W. Gregg, W. Esaias, G. Feldman, R. Frouin, S. Hooker, C. McClain and R. Woodward, Coverage opportunities for global ocean color in a multimission era, IEEE Transactions on Geoscience and Remote Sensing 36 (September 1998) 1620–1627.
[14] J. Haartsen and S. Mattisson, Bluetooth – A new low-power radio interface providing short-range connectivity, Proceedings of the IEEE 88(10) (October 2000) 1651–1661.
[15] Z. Haas, On the relaying capability of the reconfigurable wireless networks, in: *IEEE 47th Vehicular Technology Conference*, Vol. 2 (May 1997) pp. 1148–1152.
[16] D. Kahaner, C. Moler and S. Nash, *Numerical Methods and Software* (Prentice Hall, Englewood Cliffs, NJ, 1989).
[17] C. Kang and M. Golay, An integrated method for comprehensive sensor network developement in complex power plant systems, Reliability Engineering & System Safety 67 (January 2000) 17–27.
[18] F. Koushanfar et al., Global error-tolerant fault-tolerant algorithms for location discovery in ad-hoc wireless networks, UCLA Technical Report, UCLA Computer Science Department (2001).
[19] J. Lansford and P. Bahl, The design and implementation of HomeRF: A radio frequency wireless networking standard for the connected home, Proceedings of the IEEE 88(10) (October 2000) 1662–1676.
[20] K. Lieska, E. Laitinen and J. Lahteenmaki, Radio coverage optimization with genetic algorithms, in: *IEEE International Symposium on Personal, Indoor and Mobile Radio Communications*, Vol. 1 (September 1998) pp. 318–322.
[21] K. Marzullo, Tolerating failures of continuous-valued sensors, ACM Transactions on Computer Systems 8(4) (November 1990) 284–304.
[22] M. Marengoni, B. Draper, A. Hanson and R. Sitaraman, System to place observers on a polyhedral terrain in polynomial time, Image and Vision Computing 18 (December 1996) 773–780.
[23] A. Mason et al., A generic multielement microsystem for portable wireless applications, Proceedings of the IEEE 86(8) (August 1998) 1733–1746.
[24] S. Meguerdichian, F. Koushanfar, M. Potkonjak and M. Srivastava, Coverage problems in wireless ad-hoc sensor networks, in: *Proceedings of IEEE INFOCOM*, Vol. 3 (April 2001) pp. 1380–1387.
[25] A. Molina, G.E. Athanasiadou and A.R. Nix, The automatic location of base-stations for optimised cellular coverage: A new combinatorial approach, in: *IEEE 49th Vehicular Technology Conference*, Vol. 1 (May 1999) pp. 606–610.
[26] C. Nguyen, L. Katehi and G. Rebeiz, Micromachined devices for wireless communications, Proceedings of the IEEE 86(8) (August 1998) 1756–1768.
[27] N.B. Priyantha, A. Chakraborty and H. Balakrishnan, The cricket location-support system, in: *Proceedings of the Sixth Annual ACM International Conference on Mobile Computing and Networking* (August 2000) pp. 32–43.
[28] G.J. Pottie and W.J. Kaiser, Wireless integrated network sensors, Communications of the ACM 43(5) (May 2000) 51–58.
[29] A. Ralston and P. Rabinowitz, in: *A First Course in Numerical Analysis*, 2nd ed. (McGraw-Hill, New York, 1978).

[30] S. Riter and J. MacCoy, Automatic vehicle location – An overview, IEEE Transactions on Vehicular Technology, VT26(1) (February 1977).
[31] M. Shaw, P. Levin and J. Martel, The Dod: Stewards of a global information resource, the Navstar global positioning system, Proceedings of the IEEE 87(1) (January 1999) 16–23.
[32] A.H. Stroud, *Approximate Calculation of Multiple Integrals* (Prentice Hall, Englewood Cliffs, NJ, 1971).
[33] D. Tennenhouse, Proactive computing, Communications of the ACM 43(5) (May 2000) 43–50.
[34] R.A. Thisted, *Elements of Statistical Computing* (Chapman and Hall, New York, 1988).
[35] G.L. Turin, W.S. Jewell and T.L. Johnston, Simulation of urban vehicle-monitoring systems, IEEE Transactions on Vehicular Technology VT21(1) (February 1972) 9–16.
[36] R. Want and A. Hopper, Active Badges and personal interactive computing objects, IEEE Transactions on Consumer Electronics 38(1) (February 1992) 10–20.
[37] N. Yazdi, A. Mason, K. Najafi and K. Wise, A generic interface chip for capacitive sensors in low-power multi-parameter microsystems, Sensors and Actuators A (Physical) A84(3) (September 2000) 351–361.

Seapahn Megerian (Meguerdichian) is currently a Ph.D. student in the Computer Science Department at the University of California, Los Angeles. He received his computer science and engineering B.S. degree in 1998 and computer science M.S. degree in 1999 from UCLA. His primary focus is in the design and development of efficient algorithms for deployment, performance and coverage analysis, decision support, operation optimization, security, and privacy in wireless ad hoc sensor networks. In addition, his research includes high performance communication systems, system-on-chip network design, application of specific compilers, and computational security. He was the recipient of the 7th Annual International Conference on Mobile Computing and Networking (MobiCom 2001) Best Student Paper Award.
E-mail: seapahn@cs.ucla.edu

Farinaz Koushanfar has received BS degree from Sharif University of technology (1999) and MS from University of California, Los Angeles, in electrical engineering (2001). She is currently pursuing her Ph.D. at the Electrical Engineering and Computer Science Department at the University of California, Berkeley. Her research interests include various aspects of wireless sensor and information networks (in particular: location discovery, software sensor appliances and network infrastructure architecture, modeling, and distributed algorithms and optimizations), embedded systems, practical large scale optimization techniques, and intellectual property protection. She is a graduate research fellow of NSF (2000) and a recipient of the UCLA student leadership award (2001). She also received the ACM SIGMOBILE (MobiCom) best student paper award (2001).
E-mail: farinaz@eecs.berkeley.edu

Gang Qu received the B.S. and M.S. in mathematics from the University of Science and Technology of China in 1992 and 1994, and the M.S. and Ph.D. in computer science from the University of California, Los Angeles, in 1998 and 2000. He joined the Department of Electrical and Computer Engineering in the University of Maryland at College Park in 2000, where he is currently an Assistant Professor. He became a member of the University of Maryland Institute of Advanced Computer Studies in 2001. His research interests include intellectual property reuse and protection, low power system design, applied cryptography, computer-aided synthesis, and sensor networks. He won the Outstanding Master of Science Award (1998) from the Henry Samueli Engineering School in University of California, Los Angeles, and the Dimitris N. Chorafas Foundation Award (1999). He is a recipient of the 36th Design Automation Conference Graduate Scholarship Awards (1999) for his work on intellectual property protection.
E-mail: gangqu@eng.umd.edu

Giacomino Veltri is currently an undergraduate at the University of California, Los Angeles. Before transferring to UCLA, Giacomino was a student at College Of The Canyons where he was active in the community as a HITE Program Officer and an EOPS Ambassador. Giacomino first studied computers at College Of The Canyons, and as a result, became a computer programmer for WayForward Technologies, a Santa Clarita-based computer game company. In the short time during which he worked for WayForward Technologies, Giacomino has had his name associated with six different video game titles. In 1998, Giacomino graduated from College Of The Canyons and one year later he transferred to UCLA. At UCLA, Giacomino continued his study of computers as a Computer Science major, and has broadened his educational horizons by working as a research assistant for Professor Miodrag Potkonjak. Giacomino has worked on research areas such as sensor networks and general optimization, and has been involved with projects related to the maximum breach path, percolation scaling, and minimal exposure path of sensor networks, in addition to linear programming. Giacomino will receive his Bachelor's Degree in computer science in December 2001, and will begin his graduate studies in computer science at UCLA starting in 2002.
E-mail: gforce@ucla.edu

Miodrag Potkonjak is a Professor at the Computer Science Department at UCLA. He received his Ph.D. degree in electrical engineering and computer science from University of California, Berkeley, in 1991. In 1991, he joined C&C Research Laboratories, NEC USA in Princeton, NJ. Since 1995, he has been with UCLA. He has received the NSF CAREER award, OKAWA foundation award, UCLA TRW SEAS Excellence in Teaching Award and a number of best paper awards. His research interests include complex distributed systems, communication systems design, embedded systems, computational security, practical optimization techniques, and intellectual property protection.
E-mail: miodrag@cs.ucla.edu